Dr. Saprizal Turnitin Lampiran C7

by Saprizal Hadisaputra

Submission date: 24-Feb-2021 11:18AM (UTC+0700)
Submission ID: 1516754323
File name: C09.pdf (1.59M)
Word count: 5590
Character count: 26971

Monatshefte für Chemie - Chemical Monthly
https://doi.org/10.1007/s00706-020-02678-3

ORIGINAL PAPER

First solvation shell structure and dynamics of solvated Ca^{2+} in dilute aqueous ammonia by first principle approach: a QMCF MD simulation study

Niko Prasetyo[1,2] · Adi Tiara Zikri[2] · Saprizal Hadisaputra[3]

Received: 17 March 2020 / Accepted: 1 September 2020

Abstract

The investigation of solvated ion in nonaqueous or mixed solvent is a challenging task for experimental and theoretical chemistry. One of the promising approaches to elucidate the properties of solvated ion in mixed solvents is quantum mechanical charge field molecular dynamics (QMCF MD) simulation. In this study, we report the first application of QMCF MD simulation to investigate the structural and dynamical properties of solvated Ca^{2+} in 18.4% aqueous ammonia. Radial distribution function analysis showed that the average distances of Ca^{2+}–N and Ca^{2+}–O are 2.55 and 2.74 Å, respectively. The mean residence times for water and ammonia in the first solvation shell were calculated to be 2.8 and 2.74 ps, respectively. These values indicated a labile first solvation shell of Ca^{2+} in 18.4% aqueous ammonia. Meanwhile, angular distribution function analysis revealed the polyhedral structure of the first solvation shell. The average coordination numbers of 5.1 and 2.7 were obtained for water and ammonia, respectively, during the simulation. The presented simulation data provide detailed information about the properties of solvated Ca^{2+} in aqueous ammonia which will be beneficial to the investigation of the role of the ion in biological processes.

Graphic abstract

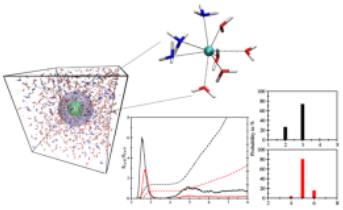

Keywords Computational chemistry · Aqueous ammonia · Molecular dynamics · Quantum chemical calculations · Ca^{2+}

Introduction

The liquid state is one of the most challenging chemical systems to investigate because it exhibits strong electrostatic forces similar to that in the solid-state and particle flexibility of the particles similar to that in the gas phase. Furthermore, most chemical reactions occur in solution. Thus, accurate experimental and theoretical methodologies to investigate the properties of the solution are necessary. One of the most challenging systems involving the liquid state is ion solvation. The structural and dynamical properties of solvated ion

✉ Niko Prasetyo
nikop@ugm.ac.id

[1] Austria-Indonesia Centre (AIC) for Computational Chemistry, Universitas Gadjah Mada, Sekip Utara, Yogyakarta 55281, Indonesia

[2] Department of Chemistry, Faculty of Mathematics and Natural Sciences, Universitas Gadjah Mada, Sekip Utara, Yogyakarta 55281, Indonesia

[3] Chemistry Education Division, Faculty of Teacher Training and Science Education, Universitas Mataram, Mataram 83125, Indonesia

Published online: 07 October 2020

represent the reactivity of the ion solution. Thus, this information is highly relevant for the treatment of specific ions, such as toxic [1], radioactive [2, 3], and essential ions [4, 5].

One of the most important essential ions is Ca^{2+}. This ion plays an important role in a large number of biological processes, for example, Ca^{2+} interacts with protein by binding to the oxygen (O) and nitrogen (N) atoms of amino acids [6]. These interactions can be investigated via molecular dynamics simulation of solvated Ca^{2+} in mixed solvents/binary mixtures containing O- and N-atoms, such as aqueous ammonia.

Several theoretical studies have been reported to explain the structural and dynamical properties of solvated Ca^{2+} in water [7, 8], liquid ammonia [9], and mixed solvents, such as acetone–water [10], DPPC–water [11], and methanol–water [12]. However, the structure of solvated Ca^{2+} in aqueous ammonia is still under discussion.

Floris et al. [13] used a classical molecular dynamics simulation report and observed preferential solvation of Ca^{2+} in an aqueous solution containing ammonia. In pure water, Ca^{2+} was solvated by eight water molecules. In contrast, in the presence of ammonia, an equilibrium between 8 and 10 coordinated ions occurred. Tongraar et al. [14] observed the polyhedral structure of the first solvation shell consisting of 5.2 water and 2 ammonia molecules through one shell quantum mechanics/molecular mechanics (QM/MM) molecular dynamics simulation. Meanwhile through classical simulation, they also observed the polyhedral structure of the first solvation shell, but consisting of 6.7 water and 3 ammonia molecules.

However, the accuracy of classical molecular dynamics simulation is still limited to the employed potentials or force fields. In one shell QM/MM simulation only the ion and the first solvation shell are treated using quantum mechanics and the empirical potentials to describe the interaction between solute and solvent in the MM region are still required. The development of the empirical potentials is a tedious task even for the interaction between monovalent ion and water, with evaluations of thousands of energy points of the respective species in the gas phase. Meanwhile, the pure QM simulation using only a few solvent molecules such as Carr–Parrinello molecular dynamics (CPMD) does not adequately represent the behavior of the bulk solution and the solvated ion. Furthermore, CPMD simulations are typically limited to density functional theory with generalized gradient approximation which is known to inadequately describe dispersive interactions [15].

The extension of the conventional QM/MM strategy [16, 17], the so-called quantum mechanical charge field molecular dynamics (QMCF MD) [18–21], is one of the prominent methods used to investigate the structural and dynamical properties of solvated ions in liquid ammonia [9, 22, 41] and aqueous ammonia [23, 24].

In the QMCF MD approach, the radius of the QM region is enlarged to fully cover the first and second solvation shells of the solute. The solute and the first solvation shell are located in Qm_{core} whereas the remaining solvent and the second solvation shell are located in QM_{layer}. The main advantage of a large QM region is the distance between solute and solvent molecules are beyond the non-Coulombic interaction cutoff distance. Thus, the empirical non-Coulombic potentials for solute solvent are not required anymore.

Furthermore, in the QMCF MD approach, the partial charges of MM atoms are embedded in the total QM Hamiltonian via external perturbation, resulting in a better description of hydrogen bonding interactions particularly those close to the border of the second solvation shell and the bulk region [18–21]. To the best of our knowledge, no reports have discussed the structural and dynamical properties of solvated Ca^{2+} in aqueous ammonia using the QMCF MD approach so far. This work aims to quantify the effect of different solute–solvent interactions on the respective structural and dynamical properties and compare the results to the pure water or liquid ammonia cases. On the basis of the QMCF MD trajectories, the structural properties are characterized by computing the associated radial and angular distribution functions (RDF and ADF) and coordination number distribution (CND). Meanwhile, the dynamical properties are evaluated based on their respective vibrational stretching of ion–ligand bonds and mean residence time (MRT).

Results and discussion

The Ca^{2+}–O and Ca^{2+}–N RDFs as well as their associated running integration obtained at a sampling time of 25 ps are depicted in Fig. 1 and the corresponding structural characteristics are listed in Table 1. A well-defined first solvation shell is observed for both ligands with the first shell maxima

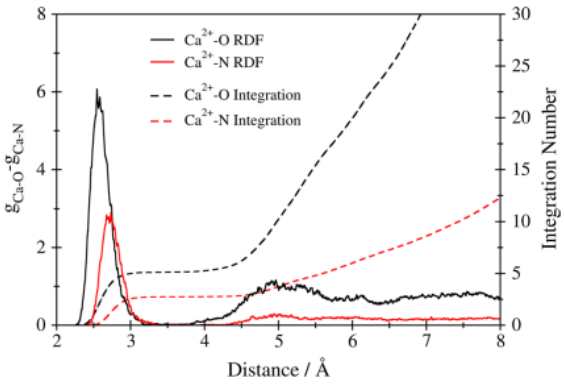

Fig. 1 RDFs of Ca^{2+}–O (black solid line) and Ca^{2+}–N (red solid line) and their respective integrations (dashed lines)

Table 1 Characteristic values for the first and second solvation shells of solvated Ca^{2+} in aqueous ammonia

	r_{L1}/Å	r_{l1}/Å	r_{L2}/Å	r_{l2}/Å	CN_1	CN_2
Ca–O	2.55	3.61	5.00	6.35	5.1	17.7
Ca–N	2.74	3.53	5.03	6.73	2.58	2.8

$r_{L,i}$ and r_{li} denote the maxima and minima in the first and second solvation shells, respectively. CN_{av},i is the average coordination number in the first and second solvation shells

Table 2 Several structural parameters of Ca^{2+} in various conditions

Method	*r* Ca–O; Ca–N/Å	CN O;N	System	References
QMCF MD simulation	2.55; 2.74	5.1; 2.58	18.4% aqueous ammonia; 298.15 K; First and second solvation shells are treated by QM method	This work
QMCF MD simulation	2.66	7.3	Liquid ammonia; 235.15 K; First and second solvation shells are treated by QM method	9
QM/MM MD simulation	2.44; 2.64	5.2; 2.0	18.4% aqueous ammonia; 298.15 K; First solvation shell is treated by QM method	14
MM MD simulation	2.48; 2.61	6.7; 3.0	18.4% aqueous ammonia; 298.15 K	13
Neutron scattering	2.56	6	40 K; Ca^{2+} in liquid ND_3	42
Neutron Diffraction	2.69	6	75 K; Ca^{2+} in liquid ND_3	27
EXAFS	2.43	6.9	$CaCl_2$ in aqueous solution	26
XRD	2.44	–	CaODA.$6H_2O$ crystal	25

r Ca–O; Ca–N is the respective Ca–O and Ca–N distances. CN is the coordination number

in the Ca^{2+}–O and Ca^{2+}–N RDFs at 2.55 and 2.74 Å, respectively. In the Ca^{2+}–O RDF, two shoulder peaks located at 2.59 and 2.6 Å are observed. Similarly, in the Ca^{2+}–N RDF, two shoulder peaks located at 2.67 and 2.7 Å are observed.

The shape of first shell RDF indicates that the ion–ligand distances underwent significant changes during simulation. In the border of the first and second solvation shells, the RDF values are only slightly above zero indicating that only a few successful ligand exchange events occurred in a comparably short simulation time of 25 ps. These observed average Ca^{2+}–O and Ca^{2+}–N distances are consistent with the experimental values employing X-ray diffraction [25], extended X-ray absorption fine structure [26], neutron diffraction [27], and neutron scattering [28, 42] (see Table 2). In comparison with the previous theoretical works that employed QMCF MD for aqueous [8]and solvated Ca^{2+} in liquid ammonia [9], the average Ca^{2+}–O and Ca^{2+}–N distances are in very good agreement reported as 2.55 and 2.66 Å, respectively.

Broad and less intense peaks with the maximum located at 4.91 Å are observed for the second solvation shell in Ca^{2+}–O RDF. Meanwhile in the Ca^{2+}–N RDF, no second solvation shell is observed. However, these second shell forms are expected because of the weak interaction between ion and ligands at a long distance. The integration of the second solvation shell RDF revealed that the major component in the second solvation shell is water.

To quantify the distribution number of water and ammonia in the first and second solvation shells, CND analysis

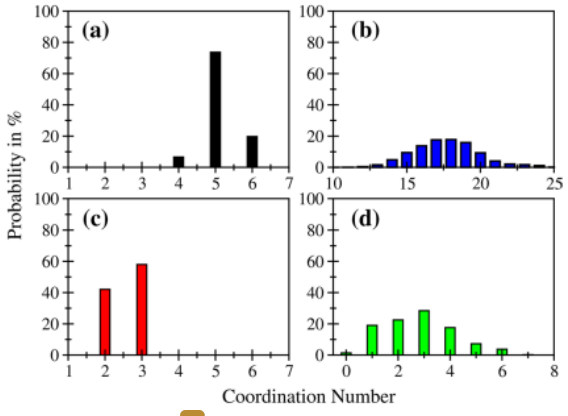

Fig. 2 CND of water the (**a**) first and (**b**) second solvation shells. CND of ammonia in the (**c**) first and (**d**) second solvation shells. All of these distributions are obtained at a sampling time of 25 ps

was conducted. The results are shown in Fig. 2. In the first solvation shell, Ca^{2+} is solvated by approximately 5.2 and 2.7 water and ammonia molecules, respectively. Meanwhile in the second solvation shell, the average coordination number is 17.7.

For both ligands, the highest occurrence probabilities in the first solvation shell are approximately 80%, indicating that no stable complexes of $[Ca(H_2O)_n]^{2+}$ or $[Ca(NH_3)_n]^{2+}$ were formed during the simulation time. This result is consistent with the RDF of the first solvation shell. Thus, the

complexes of $[Ca(H_2O)_m(NH_3)_n]^{2+}$ were formed within the short lifetime of a few picoseconds during the simulation time.

Figure 3a shows the fluctuation of the coordination number in the first and second solvation shells during the simulation time. Figure 3a also shows that the first solvation shell is flexible, and the water molecules are bonded more loosely than the ammonia molecules. The second solvation shell is more flexible with numerous ligand exchanges to bulk liquid or vice versa.

The most stable complex can be predicted qualitatively by taking the longest lifetime before the subsequent ligand exchange. Based on this criterion $[Ca(H_2O)_5(NH_3)_3]^{2+}$ is identified to have the longest lifetime of approximately 10 ps.

CND analysis confirmed that our result is consistent with those of the previously reported QM/MM MD simulation conducted by Tongraar et al. [14] which showed that Ca^{2+} was solvated by 5 H_2O and 2 NH_3 molecules.

The CND and coordination number vs time results are consistent with those of the gas-phase calculations of $[Ca(H_2O)_n]^{2+}$ and $[Ca(NH_3)_n]^{2+}$ ($n = 1$, 2, 4, 7, 8). The gas-phase calculations predicted that the interaction of Ca^{2+}–NH_3 is stronger than that of $Ca(H_2O)$. However, because of the strong repulsive forces from the dipole-oriented configuration, the coordination number of NH_3 is lower than that of H_2O. This finding is similar to that of the previous investigations of the first solvation shell structure employing a one shell QM/MM MD simulation [14].

The first solvation shell structure was elucidated using ADF analysis. The angular distribution of O–Ca^{2+}–O, O–Ca^{2+}–N, and N–Ca^{2+}–N were calculated and depicted in Fig. 4. Figure 4 shows that each angle has a broad peak ranging from 60 to 180°. Thus, rather than having a certain

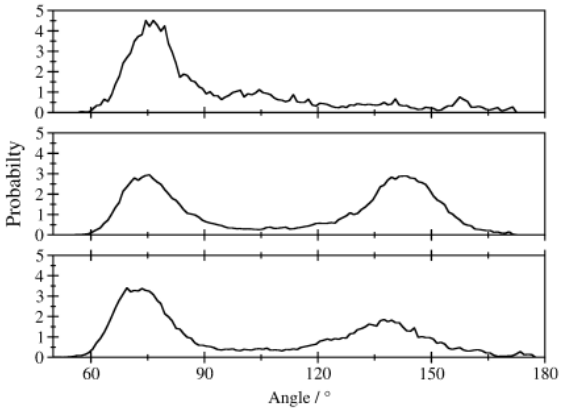

Fig. 4 ADF of (**a**) N–Ca^{2+}–N, (**b**) N–Ca^{2+}–O, and (**c**) O–Ca^{2+}–O in the first solvation shell

structural geometry, the first solvation shell of Ca^{2+} in aqueous ammonia shows a polyhedral geometry. Moreover, the broad peaks of each ADF indicate that the first solvation shell is a flexible structure. This result is consistent with the interpretation of RDF and CND results.

The narrow peak of N–Ca^{2+}–N with the maxima at 75° indicates that NH_3 is more rigid than water. The broader peak of O–Ca^{2+}–O with maximum angles of 75° and 135° indicates the flexibility and positional variability of H_2O around the ion.

The O–Ca^{2+}–N ADF shows that the arrangement of ammonia and water is distorted rather than perpendicular to each other. Overall, the ADF analysis reveals that the solvation shell structure of Ca^{2+} is polyhedral. However, the angles in the ADF analyses do not show any special pattern of certain geometries. Thus, the structural geometry of the

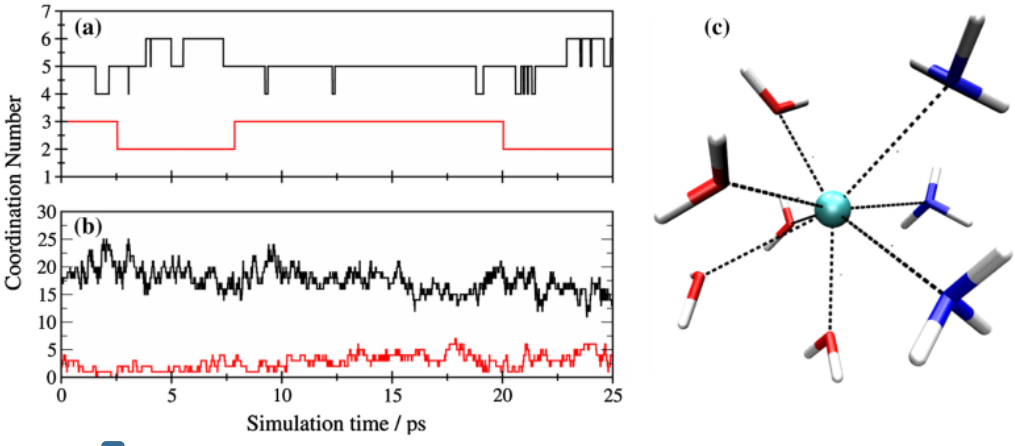

Fig. 3 Fluctuation of the coordination number in the (**a**) first and (**b**) second solvation shells (color coding: black = water; red: ammonia). **d** Snapshot of the most stable complex species of $[Ca(H_2O)_5(NH_3)_3]^{2+}$ predicted through QMCF MD simulation

first solvation shell cannot be considered to have a certain structure.

The dynamical properties of the first solvation shell are characterized by monitoring the ligand exchange events and calculating the respective MRT values. Figure 5 shows the changes of Ca^{2+}–O and Ca^{2+}–N bond distances during the simulation time. Eight successful ligand exchange events occurred for H_2O ligand whereas only two ligand exchange events were occurred for NH_3.

From the beginning of the sampling period to 8 ps, no stable complexes are formed but several complexes have coexisted. After 10 ps up to approximately 18 ps, the $[Ca(H_2O)_5(NH_3)]^{2+}$ complex is formed. At 20 ps, the complex undergoes ligand exchange events.

The quantification of the ligand exchange dynamics is achieved by computing the MRTs for both ligands in the first and second solvation shells. The MRT was calculated using direct accounting of ligand exchange events [29].

The MRT for H_2O is determined to be 12.0 ps. 7 ps, which is shorter than the computed MRT for H_2O in the first hydration shell of hydrated Ca^{2+} (16.1 ps) using a similar QMCF MD approach [8]. Meanwhile, the conventional QM/MM MD simulation overestimated the MRT for H_2O as 40 ps [7].

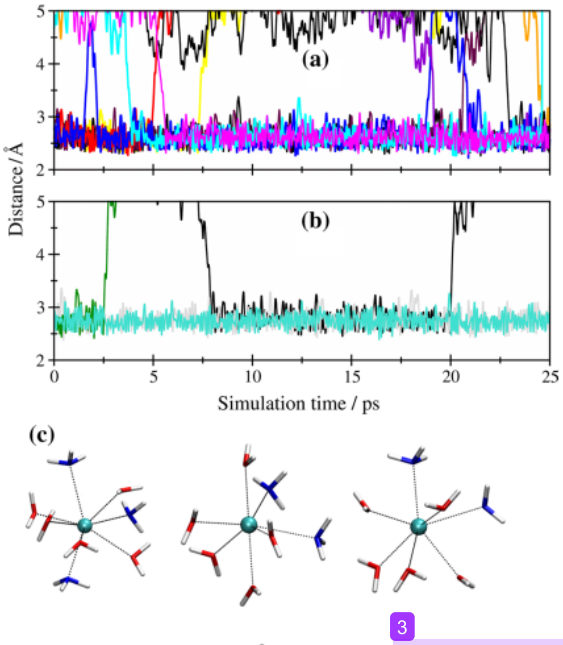

Fig. 5 Dynamics of the (**a**) Ca^{2+}–O distances in the first solvation shell. The red and yellow lines denote the dissociative exchanges during the simulation time. The purple, light blue, and blue lines showing the incoming ligands from the second solvation. (**b**) Dynamics of the Ca^{2+}–N in the first solvation shell. The green and black line denote the outcoming and incoming ligands from the second solvation shell, respectively

The MRT for NH_3 in the first solvation shell is calculated to be 21.8 ps, which is much longer than the MRT for NH_3 in the first solvation shell of solvated Ca^{2+} in liquid ammonia (12.9 ps) [7]. In the aqueous ammonia system, only 2 successful ammonia ligand exchanges are observed. In contrast, in pure liquid ammonia, 17 successful ammonia ligand exchanges are observed. Thus, our predicted MRT value is longer than the previously reported MRT for ammonia in the liquid ammonia system.

The associated rate coefficients, R_{ex} for both ligands were evaluated by comparing all of the transitions, even for the displacement time of 0 ps, with a certain number of successful ligand exchange events regardless of their displacement times. The R_{ex} values of 2 and 1 were observed for water and ammonia in the first solvation shell, respectively. These values indicated that water needs to undergo several transitions to have one successful ligand exchange event.

The ligand exchange events are shown in Fig. 5. During the simulation time of 25 ps, eight successful ligand exchange events occur for water. Of these ligand exchanges events, three of them are dissociative and the rest are associative. Meanwhile, for ammonia, three successful ligand exchange events occur. All of them are dissociative exchanges. Although an associative exchange is observed in the middle of the simulation, but the incoming ligand moves out of the first solvation shell at 20 ps. The snapshots of these exchanges are depicted in Fig. 5c. For example, ligand exchange events at 15.25, and 8 ps indicate a vivid flexible configuration of the first solvation shell.

In the second solvation shell, MRTs for H_2O and NH_3 are determined to be 2.51 and 2.27 ps, respectively. The MRT for NH_3 is slightly longer than that for pure liquid ammonia (2.08 ps) [7]. The presence of water molecules in the second solvation shell increases the strength of the hydrogen bond interaction between solvent molecules in the solvation shell, resulting in a long MRT.

The power spectra of the Ca^{2+}–O and Ca^{2+}–N vibrational stretching modes obtained via Fourier transform of the VACFs are depicted in Fig. 6. The maximum peaks of Ca^{2+}–O and Ca^{2+}–N are located at 289 and 252 cm^{-1} which corresponds to the force constants of 56.6 and 38.85 N m^{-1}, respectively. The force constant of Ca^{2+}–O is higher than that of Ca^{2+}–N indicating a stronger interaction between Ca^{2+} with water.

Although no experimental values for Ca^{2+}–O stretching vibrational spectra were reported, our Ca^{2+}–N vibrational spectra is consistent with the reported range of 250 to 370 cm^{-1} [28]. This finding confirms the appropriate setting of simulations and the selected quantum mechanical level of theory in the QMCF MD simulation.

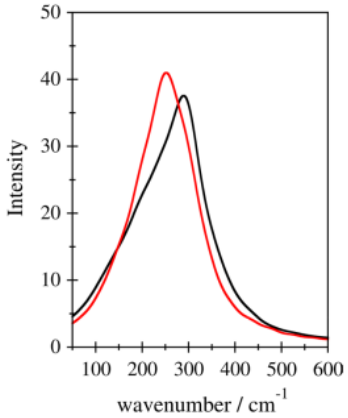

Fig. 6 Vibrational stretching of Ca^{2+}–O (black line) and Ca^{2+}–N (red line) interactions in 18% aqueous ammonia obtained via Fourier transformation of the respective VACFs of trajectories obtained by QMCF MD simulation

Conclusion

The structure and dynamics of Ca^{2+} in 18% aqueous ammonia have been successfully investigated by employing the QMCF MD simulation approach. The second solvation shell was included in the QM region and electrostatic embedding was applied to improve the description of the solvated system. Trajectories analysis showed that the labile first solvation shell had a total of 10 ligand exchange events. The most stable complex was $[Ca(H_2O)_5(NH_3)_3]^{2+}$ with an approximate lifetime of 8 ps. Direct accounting of ligand exchange events was applied to calculate MRTs of water and ammonia in the first and second solvation shells. In comparison with the MRTs for their respective pure liquid, MRTs values for water and ammonia were slightly shorter. In the second solvation shell, the MRTs for water and ammonia were short, that is, 2.51 ps and 2.27 ps, respectively.

The vibrational spectra of ion–ligand bonds are consistent with the available reported experimental data. This finding confirms the appropriate choice of level of theory to treat the QM region in QMCF MD simulation which has been highlighted by the gas-phase calculations data.

The QMCF MD simulation yielded detailed information about the structural and dynamical properties of Ca^{2+} ion in aqueous ammonia. This basic information is beneficial to the investigation of the interaction between ion and protein in biological processes. Furthermore, QMCF MD simulation provides a general approach for the investigation of the solvation of divalent, trivalent, or lanthanides cations in an aqueous or nonaqueous solvent.

Computational methodology

Quantum mechanical charge field (QMCF) MD is an enhancement of the conventional QM/MM MD. In contrast to that in the conventional QM/MM MD, the radius of the QM zone in the QMCF MD is expanded to fully cover the second hydration shell. Then, this QM region is partitioned into two subzones namely QM_{core} and QM_{layer}. The solute and the first solvation shell are located in QM_{core}, whereas the remaining solvent and the second hydration shells are located in QM_{layer}. The main advantage of this partitioning scheme is the distance between solute in QM_{core} and solvent particle in the MM region is far beyond the non-Coulombic cutoff distance. The solute and solvent particles in the MM zone interact only via electrostatic interactions. Therefore, the construction of empirical potentials for solute–solvent non-Coulombic interaction is not required anymore. For interactions between solvent particles, the empirical potentials have to be provided. Another improvement in the QMCF MD ansatz is the application of electrostatic embedding to the Hamiltonian of the QM zone. Electrostatic embedding is realized via the incorporation of atomic partial charges of MM atoms to QM Hamiltonian via an external perturbation. Thus, the QM zone is surrounded by fluctuating point charges during the simulation time and better descriptions for the interaction between QM and MM atoms are obtained, particularly in the region close to the QM–MM border.

$$V' = \sum_{i=1}^{n} \sum_{j=1}^{m} \frac{q_j^{MM}}{r_{ij}} \tag{1}$$

Because multiple sub-QM and MM regions exist in QMCF MD, the computed forces are distinguished on the basis of the respective QM regions. For example, the forces of QM_{core} are calculated using the following equation:

$$F_J^{\text{core}} = F_J^{QM} + \sum_{I=1}^{M} \frac{q_I^{MM} q_J^{QM}}{r_{IJ}^2} \left[1 + 2\frac{\varepsilon + 1}{2\varepsilon - 1} \left(\frac{r_{IJ}}{r_c} \right)^3 \right] \tag{2}$$

where F_J^{core} denotes to the quantum mechanical forces on particle J in the QM_{core} region. Meanwhile, the forces acting on the particles in the QM_{layer} and MM regions are defined using following equations:

$$F_J^{\text{layer}} = F_J^{QM} + \sum_{I=1}^{M} \frac{q_I^{MM} q_J^{QM}}{r_{IJ}^2} \left[1 + 2\frac{\varepsilon + 1}{2\varepsilon - 1} \left(\frac{r_{IJ}}{r_c} \right)^3 \right] + F_{IJ}^{nC} \tag{3}$$

$$F_J^{MM} = \sum_{\substack{I=1 \\ I \neq J}}^{N_2} \frac{q_I^{MM} q_J^{QM}}{r_{IJ}^2} + \sum_{I=1}^{N_2} F_{IJ}^{nC} \tag{4}$$

where F_J^{layer} and F_J^{MM} denote the forces acting on particles J in QM_{layer} and MM region, respectively. ensure the smooth transition between particles in the QM and MM regions, a smoothing region with a thickness of 0.2 Å was applied. The smoothed forces is described in Eq. (5):

$$F_J^{\text{smooth}} = S(r)\left(F_J^{\text{layer}} - F_J^{MM}\right) + F_J^{MM} \tag{5}$$

where S(r) denotes the smoothing function previously described in the literature [18, 19].

However, because of the large QM region in QMCF MD, the employed level of theory for QM calculations is limited to Hartree–Fock (HF) level of theory. Thus, the electron correlation effect is neglected in QMCF MD. To investigate the effect of electron correlation on simulation systems, series of gas-phase calculations of the $[Ca(H_2O)_n]^{2+}$ and $[Ca(NH_3)_n]^{2+}$ clusters (where n is the number of water or ammonia molecules. In the calculations $n = 1, 2, 4, 7$ and 8) was performed. The HF, Moller–Plesset perturbation theory second order (MP2), Becke-3 Parameter Lee–Yang–Parr (B3LYP), and Becke–Johnson damping for dispersion correction (B3LYP–D3BJ) were conducted. On the basis of the previously reported one shell QM/MM MD simulation of Ca^{2+} in aqueous ammonia, the LANL2DZ ECP [29] and DZP Dunning [31] basis sets for Ca^{2+} and water/ammonia respectively, were used for energy minimization. All gas-phase calculations were run using the ORCA QM package [43].

The results of gas-phase calculations are listed in Table 3. Based on Table 3 shows that the results of HF are close to those of MP2, whereas B3LYP significantly deviate from those of MP2. This is not surprising because the original B3LYP functional cannot describe the electrostatic interactions well and lack dispersion correction. The inclusion of dispersion correction to B3LYP (B3LYP–D3BJ) improves the obtained results, but the deviation is still higher than that of the HF level of theory. Furthermore, B3LYP is unsuitable for the investigation of the solution because it will not give a correct description of solvent at ambient temperature. Recent investigations showed that water will be described as supercooled system rather than a bulk liquid [39, 40]. Thus, the electron correlation effect does not play an important role in solvated Ca^{2+} in the aqueous ammonia system. Moreover, the application of traditional MP2 or even resolution of identity MP2 (RI-MP2) will lead to long computation times particularly when dealing with a large QM region containing up to hundreds of atom to be treated. Thus, in these simulations, the HF level of theory is selected to calculate the force and energy of QM region.

Simulation protocol

In this work, a cubic periodic simulation box containing Ca^{2+} 815 water and 184 ammonia molecules, which correspond to the 18.4% aqueous ammonia solution has been employed. The side length of the box was set to 31.74 Å, which corresponds to an experimental density of 0.927 g/cm^3 at 298.15 K. Ensemble NVT was used in all of the simulations. The long-range Coulomb interaction above 15 Å was evaluated using the reaction field method [44]. To integrate the equation of motion, a second-order Adam–Bashforth predictor–corrector was employed with a time step of 0.2 fs. BJH–CF2 water [32, 33] and ammonia models consisting of intramolecular and intermolecular potentials [34, 35] were used to describe the properties of aqueous ammonia

Table 3 Average binding energy per ligand molecule (E_{bind}) in kJ/mol and average Ca–O and Ca–N distances (rCa – O and rCa – N) in Å

HF			MP2		B3LYP		B3LYP–D3BJ	
n	E_{bind}/kJ/mol	r Ca–O/Å	E_{bind}/kJ/mol	r Ca–O/Å	E_{bind}/kJ/mol	r Ca–O/Å	E_{bind}/kJ/mol	r Ca–O/Å
1	− 214.43	2.35	− 213.59	2.36	− 223.09	2.33	− 232.92	2.33
2	− 207.69	2.37	− 207.44	2.39	− 216.31	2.36	− 222.76	2.36
4	− 190.04	2.41	− 190.79	2.42	− 197.74	2.39	− 204.64	2.39
7	− 156.04	2.51	− 160.04	2.51	− 163.18	2.49	− 174.26	2.45
8	− 145.81	2.55	− 150.62	2.54	− 152.55	2.53	− 164.35	2.50
n	E_{bind}/kJ/mol	r Ca–N/Å	E_{bind}/kJ/mol	r Ca–N/Å	E_{bind}/kJ/mol	r Ca–N/Å	E_{bind}/kJ/mol	r Ca–N/Å
1	− 234.76	2.50	− 238.95	2.52	− 253.17	2.48	− 268.61	2.48
2	− 226.35	2.54	− 230.83	2.55	− 243.43	2.51	− 253.84	2.51
4	− 202.13	2.58	− 207.15	2.59	− 215.10	2.56	− 226.81	2.55
7	− 157.57	2.72	− 166.90	2.71	− 166.94	2.70	− 181.38	2.67
8	− 143.30	2.78	− 152.84	2.75	− 152.13	2.75	− 167.36	2.72

solution. The Berendsen thermostat algorithm [45] with a relaxation time of 0.1 ps was employed to keep the temperature at 298.15 K. To avoid the 'hot solute, cold solvent' problems in the Berendsen thermostat algorithm the simulation system was rigorously equilibrated using the classical MD at least for 1 ns, followed by re-equilibration in QMCF MD for 4 ps. Finally, the sampling phase was run for 25 ps. The intermolecular potentials for the classical MD were taken from the literature [14].

The radius of QM_{core} and QM_{layer} was set to 3.5 and 6.7 Å, respectively. The smooth transitions from the QM region to the MM regions were guaranteed via a smoothing region with a thickness of 0.2 Å. All of the atomic partial charges in the QM region were calculated using the Mulliken [36] analysis every 5th step of the sampling phase. The QM calculations in QMCF MD simulations were executed using the TURBOMOLE 5.9 package [36, 37] and structural visualization was generated using VMD [38].

Acknowledgements The presented computational results have been achieved (in part) using the Austria-Indonesia Centre (AIC) for Computational Chemistry, Universitas Gadjah Mada computing facilities.

References

1. Yoshitake H (2005) New J Chem 29:1107
2. Frick RJ, Pribil AB, Hofer TS, Randolf BR, Bhattacharjee A, Rode BM (2009) Inorg Chem 48:3993
3. Frick RJ, Pribil AB, Hofer TS, Randolf BR, Bhattacharjee A, Rode BM (2009) J Phys Chem A 113:12496
4. Martonosi AN, Jona I, Molnar E, Seidler NW, Buchet R, Varga S (1990) FEBS Lett 268:365
5. Agieienko VN, Kolesnik YV, Kalugin ON (2014) J Chem Phys 140:19450
6. Chazin WJ (1995) Nat Struct Biol 2:707
7. Schwenk CF, Rode BM (2004) Pure Appl Chem 76:37
8. Lim LHV, Pribil AB, Ellmerer AE, Randolf BR, Rode BM (2009) J Comput Chem 31:1195
9. Prasetyo N, Utami W, Armunanto R, Hofer TS (2017) J Mol Liq 242:286
10. Siddique AA, Dixit MK, Tembe BL (2016) Chem Phys Lett 662:306
11. Hua W, Verreault D, Allen HC (2015) ChemPhysChem 16:3910
12. Owczarek E, Rybicki M, Hawlicka E (2007) J Phys Chem B 111:14271
13. Floris FM, Martínez JM, Tomasi J (2002) J Chem Phys 116:5460
14. Tongraar A, Sagarik K, Rode BM (2002) Phys Chem Chem Phys 4:628
15. Hofer TS, Rode BM, Pribil AB, Randolf BR (2010) Simulations of liquids and solutions based on quantum mechanical forces. In: van Eldik R, Harvey J (eds) Advances in inorganic chemistry, vol 62. Academic Press, Cambridge, p 143
16. Senn HM, Thiel W (2007) Curr Opin Chem Biol 11:182
17. Bakowies D, Thiel W (1996) J Phys Chem 100:10580
18. Rode BM, Hofer TS, Randolf BR, Schwenk CF, Xenides D, Vchirawongkwin V (2006) Theor Chem Acc 115:77
19. Hofer TS, Pribil AB, Randolf BR, Rode BM (2010) Ab initio quantum mechanical charge field molecular dynamics—a nonparametrized first-principle approach to liquids and solutions. In: Sabin JR, Brändas E, Canuto S (eds), Advances in quantum chemistry combining quantum mechanics and molecular mechanics. some recent progresses in QM/MM Method, vol 59. Academic Press, Cambridge, p 213
20. Hofer TS (2014) Pure Appl Chem 86:105
21. Weiss AKH, Hofer TS (2013) RSC Adv 3:1606
22. Hidayat Y, Armunanto R, Pranowo HD (2018) J Mol Model 24:122
23. Prasetyo N, Armunanto R (2016) Chem Phys Lett 652:243
24. Hidayat Y, Armunanto R, Pranowo HD (2018) Chem Phys Lett 699:234
25. Uchtman VA, Oertel RP (1973) J Am Chem Soc 95:1802
26. Dang LX, Schenter GK, Glezakou VA, Fulton JL (2006) J Phys Chem B 110:23644
27. Von Dreele RB, Glaunsinger WS, Bowman AL (1975) J Phys Chem 79:2992
28. Von Dreele RB, Glaunsinger WS, Chieux P, Damay P (1980) J Phys Chem 84:1172
29. Hofer TS, Tran HT, Schwenk CF, Rode BM (2004) J Comput Chem 25:211
30. Dunning TH (1970) Chem Phys Lett 7:423
31. Bopp P, Jancsó G, Heinzinger K (1983) Chem Phys Lett 98:129
32. Stillinger FH, Rahman A (1978) J Chem Phys 68:666
33. Hannongbua S, Ishida T, Spohr E, Heinzinger K (1988) Z Naturforsch A 43:572
34. Schwenk CF, Rode BM (2003) Phys Chem Chem Phys 5:3418
35. Mulliken RS (1955) J Chem Phys 23:1833
36. Ahlrichs R, Bär M, Häser M, Horn H, Kölmel C (1989) Chem Phys Lett 162:165
37. Von Arnim M, Ahlrichs R (1998) J Comput Chem 19:1746
38. Humphrey W, Dalke A, Schulten K (1996) J Mol Graph 14:33
39. Schmidt J, VandeVondele J, Kuo IFW, Sebastiani D, Siepmann JI, Hutter J, Mundy CJ (2009) J Phys Chem B 113:11959
40. Yoo S, Zeng XC, Xantheas SS (2009) J Chem Phys 130:22
41. Prasetyo N, Canaval LR, Wijaya K, Armunanto R (2015) Chem Phys Lett 619:158
42. Damay P, Leclercq F, Chieux P (1990) Phys Rev B 41:967
43. Neese F (2012) Wiley Interdiscip Rev Comput Mol Sci 2:73
44. Adams DJ, Adams EM, Hills GJ (1979) Mol Phys 38:387
45. Berendsen HJ, Postma JV, van Gunsteren WF, DiNola ARHJ, Haak JR (1984) J Chem Phys 81:3684

Dr. Saprizal Turnitin Lampiran C7

ORIGINALITY REPORT

13%	3%	13%	1%
SIMILARITY INDEX	INTERNET SOURCES	PUBLICATIONS	STUDENT PAPERS

PRIMARY SOURCES

1	Niko Prasetyo, Ria Armunanto. "Revisiting structure and dynamics of Ag + in 18.6% aqueous ammonia: An ab initio quantum mechanical charge field simulation", Chemical Physics Letters, 2016 Publication	2%
2	Muhammad Saleh, Thomas S. Hofer. "Theoretical insight on the solvation properties of Zn2+ in pure liquid ammonia: A quantum mechanical molecular charges field molecular dynamics (QMCF-MD) study", Journal of Molecular Liquids, 2020 Publication	2%
3	Wahyu Dita Saputri, Karna Wijaya, Harno Dwi Pranowo, Thomas S. Hofer. "The Jahn-Teller effect in mixed aqueous solution: the solvation of Cu2+ in 18.6% aqueous ammonia obtained from ab initio quantum mechanical charge field molecular dynamics", Pure and Applied Chemistry, 2019 Publication	2%

4	Wahyu Dita Saputri, Yuniawan Hidayat, Karna Wijaya, Harno Dwi Pranowo, Thomas S. Hofer. "Investigation of the preferential solvation and dynamical properties of Cu+ in 18.6% aqueous ammonia solution using ab initio quantum mechanical charge field (QMCF) molecular dynamics and NBO analysis", Journal of Molecular Liquids, 2019 Publication	1%
5	F. M. Floris, José M. Martínez, J. Tomasi. " Extending the polarizable continuum model to effective pair potentials in multicomponent solutions: A test on calcium–water and calcium–ammonia potentials ", The Journal of Chemical Physics, 2002 Publication	1%
6	Pilailuk Kabbalee, Anan Tongraar, Teerakiat Kerdcharoen. "Preferential solvation and dynamics of Li + in aqueous ammonia solution: An ONIOM-XS MD simulation study", Chemical Physics, 2015 Publication	1%
7	F. M. Floris. "Preferential solvation of Ca[sup 2+] in aqueous solutions containing ammonia: A molecular dynamics study", The Journal of Chemical Physics, 2002 Publication	1%

8	staff.uny.ac.id Internet Source	1%
9	Pilailuk Kabbalee, Pattrawan Sripa, Anan Tongraar, Teerakiat Kerdcharoen. "Solvation structure and dynamics of K+ in aqueous ammonia solution: Insights from an ONIOM-XS MD simulation", Chemical Physics Letters, 2015 Publication	1%
10	onlinelibrary.wiley.com Internet Source	1%
11	Hinteregger, Ernst, Andreas B. Pribil, Thomas S. Hofer, Bernhard R. Randolf, Alexander K. H. Weiss, and Bernd M. Rode. "Structure and Dynamics of the Chromate Ion in Aqueous Solution. An ab Initio QMCF-MD Simulation", Inorganic Chemistry, 2010. Publication	1%
12	"Solvation Effects on Molecules and Biomolecules", Springer Science and Business Media LLC, 2008 Publication	1%

Exclude quotes	Off	Exclude matches	< 1%
Exclude bibliography	On		